Focusing light in a curved-space

Danilo H. Spadoti, Lucas H. Gabrielli, Carl B. Poitras and Michal Lipson

Department of Electrical and Computer Engineering, Cornell University, Ithaca, NY 14853, USA
ml292@cornell.edu

Abstract: We use transformation optics to demonstrate 2D silicon nanolenses, with wavelength-independent focal point. The lenses are designed and fabricated with dimensions ranging from 5.0 μm x 5.0 μm to 20 μm x 20 μm. According to numerical simulations the lenses are expected to focus light over a broad wavelength range, from 1.30 μm to 1.60 μm. Experimental results are presented from 1.52 μm to 1.61 μm.

OCIS codes: (220.0220) Optical design and fabrication; (220.3630) Lenses

References and links

1. J. B. Pendry, "Negative Refraction Makes a Perfect Lens," Phys. Rev. Lett. **85**(18), 3966–3969 (2000).
2. H. Lee, Z. Liu, Y. Xiong, C. Sun, and X. Zhang, "Development of optical hyperlens for imaging below the diffraction limit," Opt. Express **15**(24), 15886–15891 (2007).
3. T. Matsumoto, K. S. Eom, and T. Baba, "Focusing of light by negative refraction in a photonic crystal slab superlens on silicon-on-insulator substrate," Opt. Lett. **31**(18), 2786–2788 (2006).
4. T. Asatsuma, and T. Baba, "Aberration reduction and unique light focusing in a photonic crystal negative refractive lens," Opt. Express **16**(12), 8711–8719 (2008).
5. J. Tian, M. Yan, M. Qiu, C. G. Ribbing, Y.-Z. Liu, D.-Z. Zhang, and Z.-Y. Li, "Direct characterization of focusing light by negative refraction in a photonic crystal flat lens," Appl. Phys. Lett. **93**(19), 191114–191901 (2008).
6. N. Fang, H. Lee, C. Sun, and X. Zhang, "Sub-diffraction-limited optical imaging with a silver superlens," Science **308**(5721), 534–537 (2005).
7. M. Tsang, and D. Psaltis, "Magnifying perfect lens and superlens design by coordinate transformation," Phys. Rev. B **77**(3), 035122 (2008).
8. D.-H. Kwon, and D. H. Werner, "Flat focusing lens designs having minimized reflection based on coordinate transformation techniques," Opt. Express **17**(10), 7807–7817 (2009).
9. C. A. Valagiannopoulos, and N. L. Tsitsas, "On the resonance and radiation characteristics of multi-layered spherical microstrip antennas," Electromagnetics **28**(4), 243–264 (2008).
10. U. Leonhardt, "Optical conformal mapping," Science **312**(5781), 1777–1780 (2006).
11. J. B. Pendry, D. Schurig, and D. R. Smith, "Controlling electromagnetic fields," Science **312**(5781), 1780–1782 (2006).
12. L. H. Gabrielli, J. Cardenas, C. B. Poitras, and M. Lipson, "Silicon nanostructure cloak operating at optical frequencies," Nat. Photonics **3**(8), 461–463 (2009).
13. J. Valentine, J. Li, T. Zentgraf, G. Bartal, and X. Zhang, "An optical cloak made of dielectrics," Nat. Mater. **8**(7), 568–571 (2009).
14. M. Yan, W. Yan, and M. Qiu, "Cylindrical superlens by a coordinate transformation," Phys. Rev. B **78**(12), 125113 (2008).
15. W. Wang, L. Lin, X. Yang, J. Cui, C. Du, and X. Luo, "Design of oblate cylindrical perfect lens using coordinate transformation," Opt. Express **16**(11), 8094–8105 (2008).
16. D. A. Roberts, N. Kundtz, and D. R. Smith, "Optical lens compression via transformation optics," Opt. Express **17**(19), 16535–16542 (2009).

1. Introduction

In the last decades, lenses – one of the first developed optical tools, have been intensely investigated [1], and manipulation of the trajectory of light by material engineering has seen great advances [2–9]. Some challenges in focusing light below the diffraction limit have been overcome through the use of artificial or natural metamaterials [1,2], and by negative refraction in photonic crystal [3–5]. These metamaterial lenses use negative refraction properties to focus the electromagnetic field. However, these lenses are bandwidth limited and, in addition, in optical regime, these lenses present practical limitations in fabrication [6].

Transformation optics is a technique that enables light to travel in a straight space as if it would be propagating in a curved one, by modifying the spatial distribution of the dielectric

#120945 - $15.00 USD Received 4 Dec 2009; revised 18 Jan 2010; accepted 18 Jan 2010; published 29 Jan 2010

constant accordingly [10,11]. Based on transformation optics, several demonstrations of novel optical devices were proposed and demonstrated, including cloaking devices and perfect imaging [12–15]. Since this technique does not necessarily rely on resonant structures, it is not fundamentally bandwidth limited and, therefore, could in principle enable focusing below the diffraction limit and wide bandwidth operation.

Here, we show experimentally the focusing of light using transformation optics technique in the near-infrared regime. We demonstrate a nanolens in which light propagates in a plane surface transformed into a funneled shaped, as shown in Figs. 1(a) and 1(b), respectively, similarly to the very recently proposed geometry [16]. To develop the nanolenses we employ the coordinate transformation technique similarly to the one describe in [12].

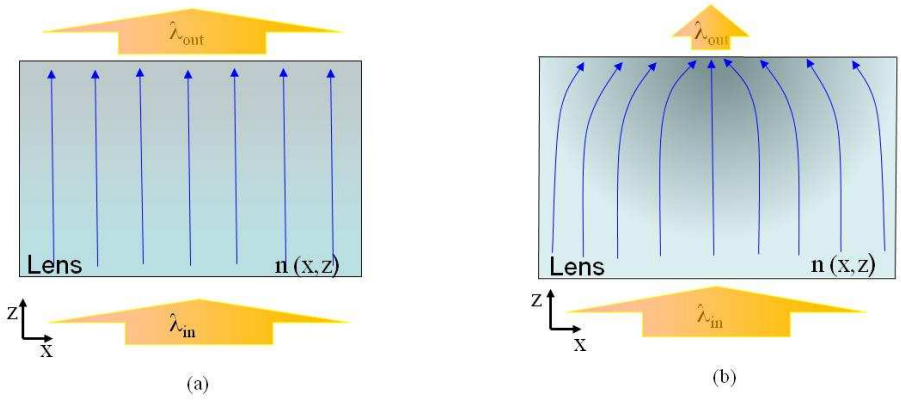

Fig. 1. Design of focusing wavelength-independent medium. (a) Conventional medium (b) Engineered medium by transformation optics, where the paths (blue lines) converge to a focal spot (FS). The arrows indicate the incident and transmitted light. The engineered medium (b) concentrates the output into a narrower region (focal spot).

2. Lenses design

In order to design the lenses, we use the space-time invariance property of Maxwell's equations to define a physical space able to function as wavelength-independent focusing medium. A grid optimization algorithm was employed to generate the transformation of coordinates [12], which define the focusing light paths and the refractive index distribution of the medium, as shown in Fig. 2(a).

The focusing of light is controlled by varying the index of refraction distribution on the medium. The lens structure, with gradient refractive index varying between 1.0 (air) and 3.5 (silicon) was first generated, as shown in Fig. 2(a). Afterward, using the same density of index distribution previous calculated, the structure was discretized and a pattern of holes (air) in silicon was generated, as shown in Fig. 2(b). The pattern of holes in the silicon will be use to fabricate the lenses. Note that the density of the refractive index in the continuous and discrete structures showed, respectively, in Figs. 2(a) and 2(b), is the same.

#120945 - $15.00 USD Received 4 Dec 2009; revised 18 Jan 2010; accepted 18 Jan 2010; published 29 Jan 2010

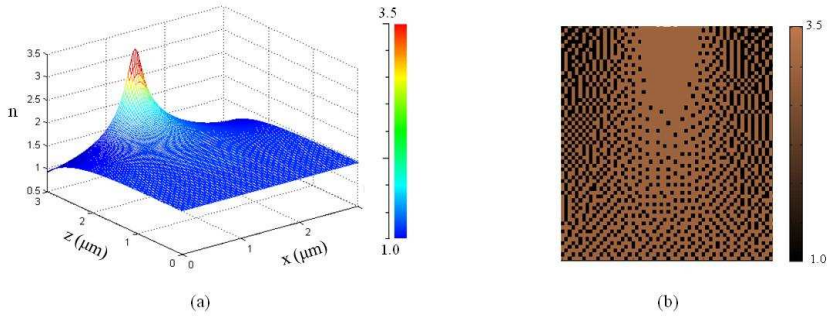

Fig. 2. (a) Lens with continuous refractive index distribution. (b) Lens with discrete index profile, black color represents air-holes and brown, silicon.

We use finite-difference time-domain and beam propagation methods to simulate light propagation in the index profiles shown in Figs. 2(a) and 2(b). The silicon absorption loss is included in the simulations. The source light is considered TM-polarized, with the major component of the electric field perpendicular to the device plane, and with wavelengths, λ, varying from 1.30 μm to 1.60 μm. Figures 3 and 4 show the amplitude of the electric field propagating in the z direction. In Figs. 3(a) and 3(b) a continuous refractive index medium is investigated, for an incident light with λ = 1.30 μm and λ = 1.55 μm, respectively. Figures 4(a) and 4(b) show the same plot depicted in Figs. 3(a) and 3(b), but for discrete refractive index distribution (80 nm air holes in Si). As shown in figures below, the focusing effect is clear, and its position is independent of the wavelength, which can also be seen at the power intensity plots (blue lines) measured in the center of the device (X = 0).

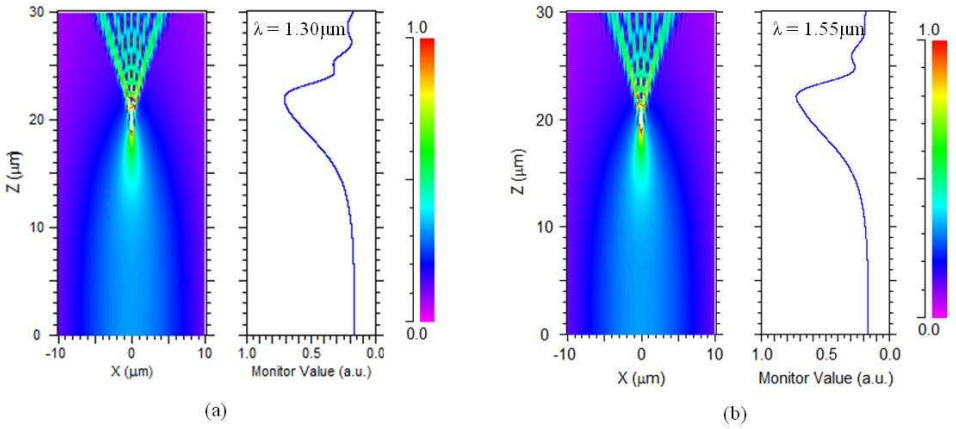

Fig. 3. Amplitude of the field for lens with dimensions 20 μm x 20 μm, and with homogeneous index distribution (as in Fig. 2(a)): (a) λ = 1.30 μm, (b) λ = 1.55 μm.

#120945 - $15.00 USD Received 4 Dec 2009; revised 18 Jan 2010; accepted 18 Jan 2010; published 29 Jan 2010

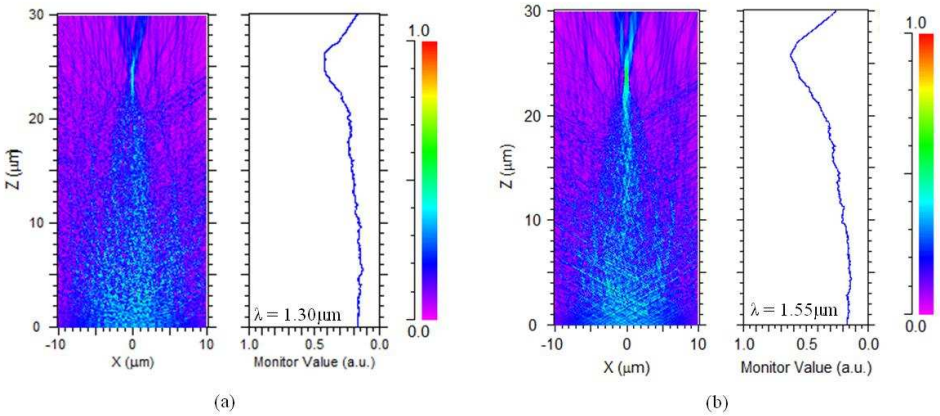

Fig. 4. Amplitude of the field for lens with dimensions 20 μm x 20 μm, and with discrete index distribution (as shown in Fig. 2(b)): (a) λ = 1.30 μm, (b) λ = 1.55 μm.

From Fig. 4, it is possible to observe that the air holes in the device lead to additional light scattering when compared to the results from Fig. 3. One can see that, as the wavelength is decreased, a stronger scattering occurs as expected from Rayleigh scattering. Furthermore, closer to 1.30 μm the silicon absorption increases. These two factors combined result in the power reduction observed in the focusing region on the line plot of Fig. 4(a).

The distance from the output of the lens to the focal point does not depend on the input wavelength. Note that this is in contrast to, for example, Fresnel lens, where the focal distance is, approximately, $f \approx 1/\lambda$. To support the wavelength independence of the focusing spot in the z direction, we used a Finite-Difference Time-Domain (FDTD) algorithm to simulate light propagation in different device sizes for a range of wavelengths in the discrete medium. The resulting power intensity in the center of the device versus propagation distance, for wavelengths from 1.45 μm to 1.60 μm, are presented in Fig. 5, showing little to no spectral dependence.

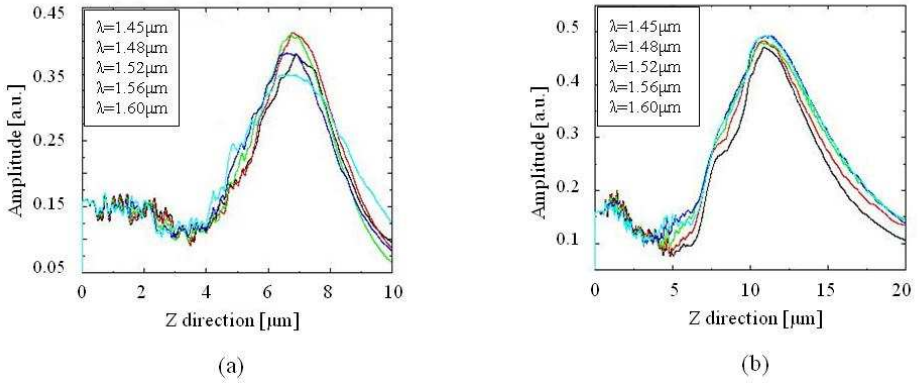

Fig. 5. Power intensity distribution for a lens with discrete index refraction and focal spot equal to 35% of the width. Lens dimension: (a) 5 μm x 5 μm, (b) 10 μm x 10 μm.

When using transformation optics, the focal spot (FS) dimension is, in principle, not fundamentally limited to the wavelength of light. However, here, it is limited by the refractive index of the silicon. The higher the refractive index available, the narrower the focal spot, and, therefore, the higher the concentration that can be obtained. The concentrator factor, C, is the relation between the expected power density at the focusing region when the input edge of the

#120945 - $15.00 USD Received 4 Dec 2009; revised 18 Jan 2010; accepted 18 Jan 2010; published 29 Jan 2010

lens is illuminated by a plane wave, and the power density of the plane wave. For both lenses in Fig. 5 the concentration factor is, approximately, 2.8.

3. Experimental Results

The lens theoretically studied in the previous section was fabricated using standard CMOS technology and experimentally investigated using near-field scanning optical microscopy (NSOM). The discrete index profile of the lens shown in Fig. 2(b) was patterned in a silicon-on-insulator (SOI) wafer using single step electron beam lithography on a 60nm layer of Dow Corning® XR-1541 resist. The 80 nm holes were etched using a standard Cl_2 inductively coupled plasma process. A scanning electron microscope (SEM) image of the fabricated lens with 10 μm by 10 μm is shown in Fig. 6. One can see the varying density of air holes in different regions of the device, with almost no holes present at the center of the focusing edge.

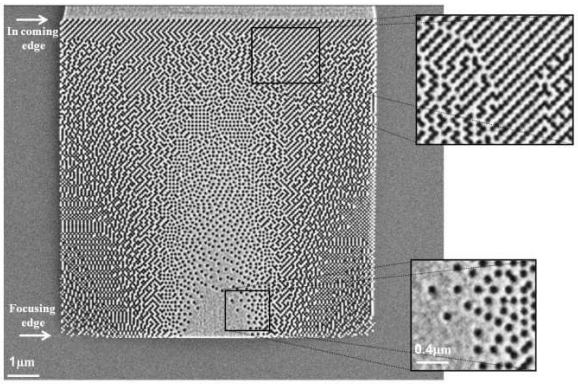

Fig. 6. Scanning electron microscope of a fabricated lens with dimension 10 μm x 10 μm. 80nm air-holes are etched in SOI wafer with varying density determine the distribution of the effective index of the lens. The distribution of the air holes is given by the design shown in Fig. 2(b). Also shown are SEMs of the incoming edge area and in the focusing edge area.

Using a NSOM tip with 500 nm aperture we scanned the lens in the x-z plane to measure the light propagation profile. Light was incident through a waveguide 450 nm wide. At the end of the waveguide a taper was used to connect the waveguide with the lens (see Fig. (7a)). The measurements for wavelengths with 1.52 μm, 1.55 μm and 1.61 μm are displayed in Figs. 7(b), 7(c) and 7(d), respectively. Additionally, below the images, a profile of the light intensity right outside the focusing edge of the lens is shown. The FWHM of the intensity distribution in the edge of the lenses (where the focal length was designed to be located in Fig. 1(b)) is approximately 2 μm. The asymmetry observed in the distribution of light in the device (Fig. 7) is due to the multimode nature of the input taper, and not because of the asymmetric disposition of the air holes. The placement of the holes should not affect the transmission pattern since only the average dielectric constant is affecting light propagation.

#120945 - $15.00 USD Received 4 Dec 2009; revised 18 Jan 2010; accepted 18 Jan 2010; published 29 Jan 2010

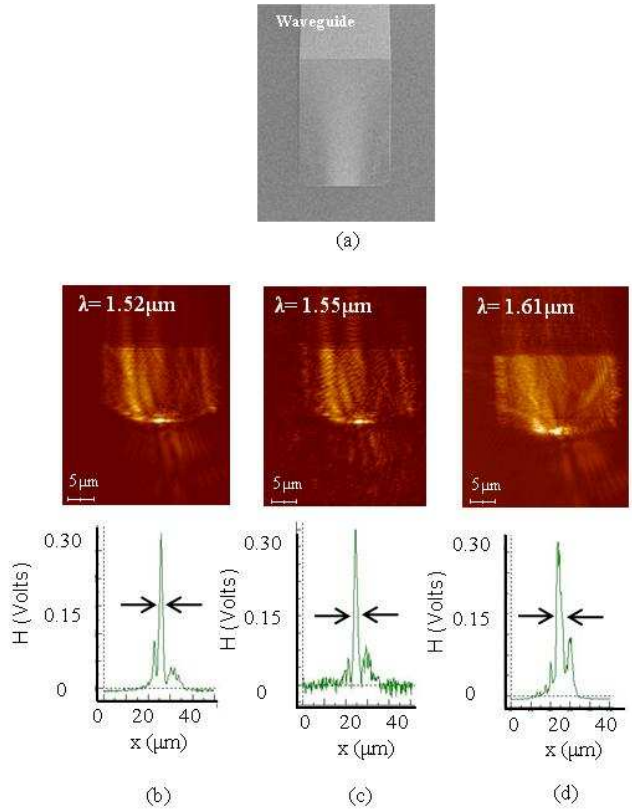

Fig. 7. (a) SEM of the lens; NSOM images for 20 μm x 20 μm lens dimension, FS = 7μm, for three different input wavelengths: (b) λ = 1.52 μm (c) λ = 1.55 μm (d) λ = 1.61 μm. The plots in green represent the power intensity measured at the output of the sample.

4. Conclusion

In this work a silicon nanolens obtained using transformation optics was demonstrated. The lens presents a wavelength-independent focal point, and could enable a great versatility and a wide variety of applications in integrated optics, such as, coupling between waveguides, and devices with small modal volume for detection and modulation.

Acknowledgements

The authors would like to acknowledge the support of Cornell's Center for Nanoscale Systems (CNS) which is funded by the National Science Foundation, and the Brazilian Federal Agency for Support Evaluation of Graduate Education (CAPES). This work was performed in part at the Cornell Nanoscale Facility, a member of the National Nanotechnology Infrastructure Network, which is supported by the National Science Foundation. This work made use of the Molecular, Optical, and Cellular Surface Imaging facility of the Cornell Center for Materials Research (CCMR) with support from the National Science Foundation Materials Research Science and Engineering Centers (MRSEC) program (DMR 0520404).

#120945 - $15.00 USD Received 4 Dec 2009; revised 18 Jan 2010; accepted 18 Jan 2010; published 29 Jan 2010